AIP | Physics of Fluids

# Scale growth of structures in the turbulent boundary layer with a rod-roughened wall

Jin Lee, Jung Hoon Kim, and Jae Hwa Lee

Citation: Physics of Fluids **28**, 015104 (2016); doi: 10.1063/1.4939714
View online: http://dx.doi.org/10.1063/1.4939714
View Table of Contents: http://scitation.aip.org/content/aip/journal/pof2/28/1?ver=pdfcov
Published by the AIP Publishing

**Articles you may be interested in**

Numerical simulations of sink-flow boundary layers over rough surfaces
Phys. Fluids **26**, 015113 (2014); 10.1063/1.4862672

Turbulent boundary layer flow subject to streamwise oscillation of spanwise wall-velocity
Phys. Fluids **23**, 081703 (2011); 10.1063/1.3626028

Wall pressure fluctuations beneath supersonic turbulent boundary layers
Phys. Fluids **23**, 085102 (2011); 10.1063/1.3622773

Inner/outer layer interactions in turbulent boundary layers: A refined measure for the large-scale amplitude modulation mechanism
Phys. Fluids **23**, 061701 (2011); 10.1063/1.3589345

Incompatibility of the exponential scaling law for a zero pressure gradient boundary layer flow with Reynolds averaged turbulence models
Phys. Fluids **17**, 048105 (2005); 10.1063/1.1879053


This article is copyrighted as indicated in the article. Reuse of AIP content is subject to the terms at: http://scitation.aip.org/termsconditions. Downloaded to IP: 114.70.8.215 On: Wed, 13 Jan 2016 01:20:18

CrossMark click for updates

PHYSICS OF FLUIDS **28**, 015104 (2016)

# Scale growth of structures in the turbulent boundary layer with a rod-roughened wall

Jin Lee,[1] Jung Hoon Kim,[2] and Jae Hwa Lee[2,a)]
[1]*Department of Mechanical Engineering, Johns Hopkins University, 3400 N. Charles St., Baltimore, Maryland 21218, USA*
[2]*School of Mechanical and Nuclear Engineering, Ulsan National Institute of Science and Technology (UNIST), 50 UNIST-gil, Ulsan 689-798, South Korea*

(Received 11 June 2015; accepted 19 December 2015; published online 12 January 2016)

Direct numerical simulation of a turbulent boundary layer over a rod-roughened wall is performed with a long streamwise domain to examine the streamwise-scale growth mechanism of streamwise velocity fluctuating structures in the presence of two-dimensional (2-D) surface roughness. An instantaneous analysis shows that there is a slightly larger population of long structures with a small helix angle (spanwise inclinations relative to streamwise) and a large spanwise width over the rough-wall compared to that over a smooth-wall. Further inspection of time-evolving instantaneous fields clearly exhibits that adjacent long structures combine to form a longer structure through a spanwise merging process over the rough-wall; moreover, spanwise merging for streamwise scale growth is expected to occur frequently over the rough-wall due to the large spanwise scales generated by the 2-D roughness. Finally, we examine the influence of a large width and a small helix angle of the structures over the rough-wall with regard to spatial two-point correlation. The results show that these factors can increase the streamwise coherence of the structures in a statistical sense. © *2016 AIP Publishing LLC.* [http://dx.doi.org/10.1063/1.4939714]

## I. INTRODUCTION

Experimental and numerical studies have shown that long structures in the log layer play a crucial role in the generation and transport of streamwise turbulent kinetic energy and Reynolds shear stress in canonical smooth-wall-bounded turbulent flows.[1–3] These structures correspond to bulges or hairpin packets of large-scale motions (LSMs) with streamwise extents on the order of 1-3$\delta$ and very-large-scale motions (VLSMs) with sizes in the range of 10-30$\delta$, where $\delta$ is the boundary layer thickness.[1–6]

Hairpin packets consist of a coherent group of hairpin vortices aligned along the streamwise direction.[5] These structures create elongated low-momentum regions beneath them which are bounded in the spanwise direction by high-momentum regions.[1,5,7] Streamwise velocity fluctuating structures on a very large scale were initially visualized in an experimental study[2] with a spanwise rake consisting of 10 hot-wires. They showed that very long meandering positive and negative streamwise velocity fluctuations on the order of $O(20\delta)$ are characterized by meandering motions in the log layer, creating an X-shaped pattern in a two-point spatial correlation. In a direct numerical simulation (DNS) study of a smooth-wall turbulent pipe flow, Baltzer *et al.*[8] found a consistent X-shaped pattern at a low contour level of correlation. However, using conditional averages given low-momentum events, they showed that the X-shaped correlation is due to the concatenation of streamwise-aligned LSMs with a spanwise offset along dominant helix angles of 0° and 4°–8° relative to the streamwise direction. They interpreted that the apparent wavering of the VLSM on a scale of O(6$\delta$) in the turbulent boundary layer (TBL) is induced as a consequence of spanwise offset LSMs rather than through sinusoidal perturbation of an otherwise straight, streamwise-aligned sequence

a)Author to whom correspondence should be addressed. Electronic mail: jhlee06@unist.ac.kr. Tel.: 82-52-217-2350. Fax: 82-52-217-2408.

 ©2016 AIP Publishing LLC

This article is copyrighted as indicated in the article. Reuse of AIP content is subject to the terms at: http://scitation.aip.org/termsconditions. Downloaded to IP: 114.70.8.215 On: Wed, 13 Jan 2016 01:20:18

of LSMs. Through time-evolving instantaneous fields, Lee and Sung[6] and Lee *et al.*[9] provided clear evidence of the formation of VLSM in which adjacent packet-type structures combine to form VLSM on the order of $O(18\delta)$, as conjectured by Kim and Adrian.[10]

Due to the significant importance of LSMs in wall-bounded turbulent flows, extensive studies of structures over rough-wall TBLs have been performed.[11–14] Wu and Christensen[13] carried out a particle image velocimetry (PIV) experiment with the realistic roughness of an actual turbine blade, focusing on the log layer, which is nearly the outer edge of the roughness sublayer ($y = 0.15\delta = 4k$, where $k$ is the roughness height). They showed that hairpin vortex packets exist in the outer layer of a rough-wall flow, contributing heavily to the Reynolds shear stress, consistent with a smooth-wall flow. Furthermore, they demonstrated that the streamwise length scale of low-momentum regions measured by streamwise two-point correlations at a level of 0.3 is reduced in the presence of roughness, similar to earlier results by Krogstad and Antonia[11] with a threshold 0.3 and Volino *et al.*[12] with a threshold 0.5 for turbulent flows over mesh-type roughness. Wu and Christensen[13] suggested that the streamwise shortening of the turbulence scales is most likely due to (1) a reduction in the streamwise spacing of consecutive vortices in vortex packets, as supported by Lee *et al.*;[14] (2) a modification of the spanwise meandering nature of LSMs, as inferred based on work by Hutchins and Marusic;[2] and (3) the emergence of abundant isolated vortical structures generated by roughness.

For regularly arranged 2-D rod-roughened walls, Volino *et al.*[15,16] found that while the inclination angles and shapes of correlations are similar irrespective of the wall condition, the streamwise and wall-normal extents of correlations at a contour level of 0.5 are approximately 40% larger than in the smooth-wall case. They attributed the increase to large-scale attached motions generated by much larger scales of structure originating from the width of the roughness elements. It should be noted that for roughness from a surface scan of a turbine blade when $k = 2.1$ mm ($\delta/k = 50$), the streamwise extent of the streamwise two-point correlation was enhanced in the log layer, whereas it is decreased for the same roughness when $k = 4.2$ mm ($\delta/k = 28$).[17] However, the correlation over the 2-D surface roughness was shown to be elongated in the streamwise direction regardless of roughness size (e.g., $\delta/k = 32$ and 161) in the experimental study.[16]

Except for studies with significant scale separation (e.g., $\delta/k \gg 1$[18]), Mejia-Alvarez *et al.*,[19] for the first time to the best of the authors' knowledge, explore the spatial features of very long meandering motions in a TBL overlying irregular roughness with moderate scale separation ($\delta/k \sim 24$), although the measurement was carried out at $y = 0.065\delta = 1.56k$ (not log region). Because the PIV field of view was $0.45\delta^* 0.46\delta$ on the $xz$-plane, elongated streamwise fields of view for long motions were reconstructed using Taylor's hypothesis. They showed that signatures of very long negative streamwise fluctuating structures are consistent with those over a smooth-wall flow and that low-momentum regions extend to several boundary layers thickness in the streamwise direction. However, because the measurement was performed at a fixed position with Taylor's hypothesis, there were limitations when examining the variation of a low-momentum region with advection along the downstream with a possible incorrect interpretation of LSMs or VLSMs in highly sheared regions, especially over the rough-wall.[20,21] One means of overcoming these limitations without using Taylor's hypothesis is high-resolution DNS, which can provide full volumetric three-dimensional data, while the Reynolds number in DNS is much lower than that in experiments.

In the present study, a DNS of a TBL with surface roughness is performed with a long computational domain to examine the possible cause of the streamwise scale growth of structures. The roughness is numerically designed to have the form of 2-D square-edged spanwise rods which are periodically arranged in the streamwise direction with a streamwise pitch of $\lambda = 8k\ (= 12\theta_{in})$ and a roughness height of $k = 1.5\theta_{in}$. Because LSMs and VLSMs are often populated in the log layer over a smooth-wall,[2] our attention is primarily given at about $y/\delta = 0.15$ (the upper limit of the log layer). Under the present roughness configuration, the depth of the roughness sublayer corresponds approximately to $y/\delta = 0.25$ and 0.954 based, respectively, on $y = 5k$ and $y = 3k_s$;[22] thus, it can be expected that long structures in the log layer are directly affected by the surface roughness, where $k_s$ is the sand grain roughness height. We initially examine instantaneous flow fields and streamwise two-point spatial correlations to gain some idea about the spatial features of long elongated structures of negative streamwise velocity fluctuations. Then, time-evolving instantaneous fields are analyzed to investigate the spatial dynamics of these structures for streamwise scale growth over a rough-wall.

This article is copyrighted as indicated in the article. Reuse of AIP content is subject to the terms at: http://scitation.aip.org/termsconditions. Downloaded to IP: 114.70.8.215 On: Wed, 13 Jan 2016 01:20:18

Finally, a hairpin model is employed to construct a synthetic very long region with negative momentum, after which the influence of the helix angle and the spanwise width of the structures on the streamwise coherence of the two-point correlation is examined.

## II. NUMERICAL METHOD

For an incompressible TBL flow, the Navier-Stokes and continuity equations in Cartesian coordinates are employed as governing equations,

$$\frac{\partial u_i}{\partial t} + \frac{\partial u_i u_j}{\partial x_j} = -\frac{\partial p}{\partial x_i} + \frac{1}{Re}\frac{\partial^2 u_i}{\partial x_j \partial x_j} + f_i, \tag{1}$$

$$\frac{\partial u_i}{\partial x_i} = 0. \tag{2}$$

Here, $x_i$ are the Cartesian coordinates and $u_i$ are the corresponding velocity components. All variables are non-dimensionalized by the free-stream velocity ($U_\infty$) and the momentum thickness at the inlet ($\theta_{in}$), and the inlet Reynolds number is defined as $Re_\theta = U_\infty \theta_{in}/\nu$, where $\nu$ is the kinematic viscosity. The equations are integrated in time using the fractional step method along with an implicit velocity-decoupling procedure.[23] Block LU decomposition based on approximate factorization is applied to achieve both velocity-pressure decoupling and the decoupling of intermediate velocity components. In this approach, the terms are first discretized in time using the Crank-Nicholson method, and the coupled velocity components are then solved without iteration. All terms are resolved using a second-order central difference scheme in space with a staggered mesh. In order to describe the roughness element with Cartesian coordinates and a rectangular domain, the immersed boundary method is used.[24] The discrete-time momentum forcing $f_i$ is calculated explicitly in time to satisfy the no-slip condition at the immersed boundary using the previous velocity field near the forcing point. The numerical code employed in the present study is the same as used in our previous study with the same roughness configuration with shorter streamwise computational domain.[25]

The notation adopted is such that $x$, $y$, and $z$ denote the streamwise, wall-normal, and spanwise coordinates, respectively, and that $u$, $v$, and $w$ denote the corresponding velocity components. The domain size and mesh resolution are summarized in Table I. The computational domain in each direction ($L_x \times L_y \times L_z$) is $1152\theta_{in} \times 60\theta_{in} \times 80\theta_{in}$, where the corresponding mesh size is $3073 \times 150 \times 513$, and the grid resolutions are $\Delta x^+ = 6.0$, $\Delta {y_{min}}^+ = 0.2$, and $\Delta z^+ = 3.0$, respectively. Although not shown here, a grid sensitivity study with doubled and quadruple resolutions for computational feasibility indicates that the influence of the mesh resolution is negligible in the present simulation. Because experimental and numerical studies have suggested the existence of VLSMs in TBLs with a maximum streamwise length up to $\sim 20\delta$,[2,6] the streamwise domain size here is set to $1152\theta_{in}$ ($>150\delta_{in}$, where $\delta_{in}$ is the inlet boundary layer thickness). In addition, in order to compare the rough-wall flow with a smooth-wall flow at a similar Reynolds number, a simulation for a smooth-wall is also performed with a longer streamwise domain length of $1920\theta_{in}$ due to small increasing rate of the boundary layer thickness. An analysis of two-point spatial correlation confirms that the domain size in the streamwise and spanwise directions are adequate based on the convergence of the correlation to zero within the domain size. Non-uniform grid distributions are employed in the wall-normal direction by using the hyperbolic tangent function and a uniform grid distribution in both the streamwise and spanwise directions.

The no-slip boundary condition is imposed at the solid wall, and the boundary conditions on the top surface of the computational domain are $u = U_\infty$ and $\partial v/\partial y = \partial w/\partial y = 0$. Periodic boundary conditions are applied in the spanwise direction. Since the boundary layer is spatially developing in

TABLE I. Domain size and mesh resolution.

| | $Re_{\theta_{in}}$ | $L_x/\theta_{in}$ | $L_y/\theta_{in}$ | $L_y/\theta_{in}$ | $N_x, N_y, N_z$ | $\Delta x^+$ | $\Delta z^+$ | $\Delta {y_{min}}^+$ | $\Delta t U_\infty/\theta_{\text{in}}$ |
|---|---|---|---|---|---|---|---|---|---|
| Smooth | 300 | 1920 | 60 | 80 | 5121, 150, 257 | 6.0 | 5.0 | 0.2 | 0.1 |
| Rough | 300 | 1152 | 60 | 80 | 3073, 150, 257 | 6.0 | 5.0 | 0.2 | 0.1 |

This article is copyrighted as indicated in the article. Reuse of AIP content is subject to the terms at: http://scitation.aip.org/termsconditions. Downloaded to IP: 114.70.8.215 On: Wed, 13 Jan 2016 01:20:18

the downstream direction, realistic inflow data of rough-wall turbulent flow are required at the inlet with an adequate boundary condition at the outlet. However, because it is impossible to accurately generate a turbulent inflow characteristic of flow over a rough-wall, DNS of flow over a rough-wall must use a smooth-wall inflow, leading to a step change from a smooth to a rough-wall. An auxiliary simulation for the inlet boundary condition over a smooth-wall is carried out based on recyling method[26] at $Re_\theta = 300$. Although not shown here, comparison of turbulent statistics of mean velocity and turbulent stresses with previous DNS data[27] shows an excellent agreement with the present results. The convective boundary condition at the exit is specified as $(\partial u/\partial t) + c(\partial u/\partial x) = 0$, where $c$ is the local bulk velocity. For more detailed information, the readers can refer to our previous papers.[14,25]

## III. RESULTS AND DISCUSSION

Figure 1 shows streamwise velocity fluctuating structures in the log layer through the entire domain. Here, the virtual origin is considered to depict the wall-normal distance from the wall using the Jackson's definition,[28] and $u^+ (= u'/u_\tau)$ is the streamwise velocity fluctuations ($u'$) normalized by the friction velocity $u_\tau$. Near the inlet, the flow travels downstream over the smooth-wall, and the surface condition changes from a smooth to a rough surface at $x/\theta_{\text{in}} = 80$. After the step change, it is clear that high- and low-momentum regions are significantly activated in the logarithmic layer. The transient region in the range of $80 \le x/\theta_{\text{in}} \le 300$ is defined based on our previous analysis using boundary layer parameters, and first- and second-order statistics.[14,25,29] In particular, Lee[29] found that there occurs significant interaction of hairpin vortices through the transient region, creating spanwise scale growth of the hairpins along the downstream over the rough-wall. The further downstream region is defined as the equilibrium region, in which the self-preservation form of turbulent statistics is established. In the present study, long structures in the equilibrium region are analyzed to examine their streamwise-scale growth mechanism over the rough-wall.

For a clear characterization of the long motions in Fig. 1, Gaussian filtering and spectral filtering are applied to the instantaneous flow fields over the rough- and smooth-walls. The Gaussian filtering is useful for averaging small-scale features of structures,[6] and the spectral filtering based on a spanwise cutoff wavelength allows to divide large-scale structures from small-scale structures.[30,31] The result for the rough-wall TBL over the $20\delta$ long domain (within the equilibrium region) is shown in Fig. 2(a), and the corresponding motions over a smooth-wall are plotted in Fig. 2(b) with the same filtering methods. It is obvious that the streamwise domains of the present simulations over the rough- and smooth-walls include a number of long negative $u'$ streaks (blue color) in the log layer with multiple scales around them with varying strengths. In particular, the thick dashed lines drawn on four prominent examples of the negative $u'$-streaks over the smooth-wall in Fig. 2(b) demonstrate that the long motions of the negative streamwise velocity fluctuations are inclined to the spanwise direction with helix angles at approximately 4°–7°, consistent with a previous observation in a turbulent pipe flow with a smooth-wall.[8] For the rough-wall data in Fig. 2(a), the general features of the structures appear to be similar to the smooth-wall data, except for a more streamwise-aligned pattern with a helix angle of 0°–4° and a slightly larger spanwise width. It should be noted that while the above spatial characteristics over the rough- and smooth-walls do not appear in every instantaneous field, such a feature is very commonly observed.

In Fig. 3, we calculate the spatial two-point correlation of the streamwise velocity fluctuations in the log layer to provide the statistical properties of structures over both rough- and smooth-walls. The two-point correlation is defined as follows: $R_{uu}(x, r_z) = \langle u'(x_r, z)u'(x, z + r_z)\rangle / \sigma_{u'}^2$, where $x_r$

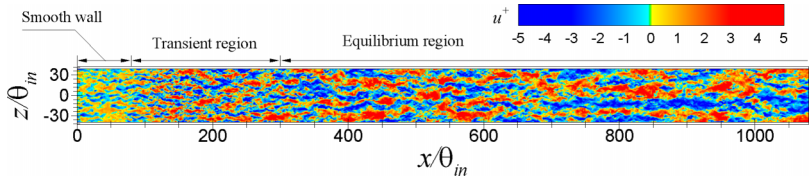


FIG. 1. Streamwise velocity fluctuating structures on the horizontal plane (at $y'(= y - \varepsilon)/\delta = 0.147$) over the entire computational domain. Here, $\varepsilon$ is the virtual origin extracted in the middle of the entire domain (at $x/\theta_{in} = 576$).

This article is copyrighted as indicated in the article. Reuse of AIP content is subject to the terms at: http://scitation.aip.org/termsconditions. Downloaded to IP: 114.70.8.215 On: Wed, 13 Jan 2016 01:20:18

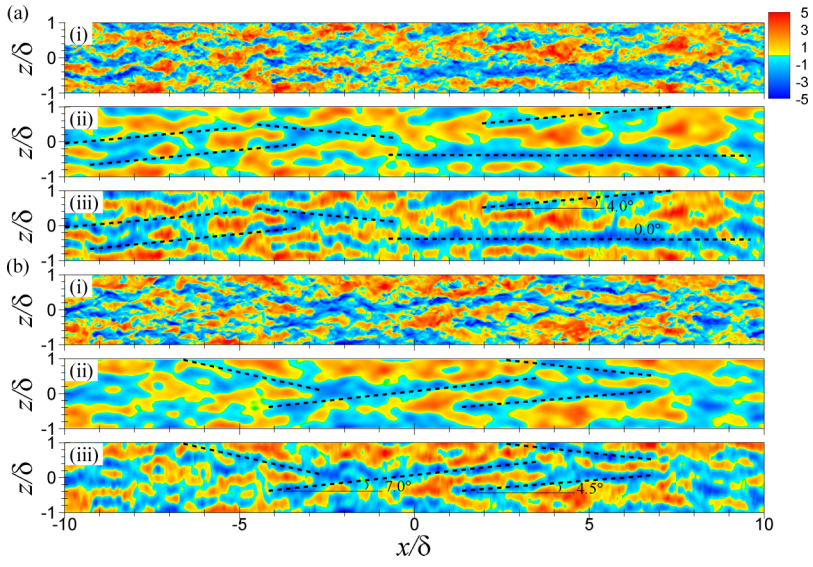


FIG. 2. Visualization of the instantaneous fields with a focus on very long $u'$-structures over (a) rough- and (b) smooth-walls at $y'/\delta = 0.147$ (within the roughness sublayer). (i) Raw data, (ii) Gaussian-filtered data with filter size $= \delta/2 \times \delta/2$, and (iii) spectral-filtered data with a cutoff spanwise wavelength of $\lambda_z/\delta > 0.5$. In each figure, $\delta$ is extracted in the middle of the present figures, and the Reynolds numbers are varied in the range of $Re_\theta = 930$–$1800$ and $Re_\theta = 1046$–$1450$ for the rough- and smooth-walls, respectively. Thick dashed lines indicate the helix angles of the structures over the rough- and smooth-walls.

is the streamwise reference location, $r_z$ is the spatial separation in the $z$ direction, and $\sigma_{u'}$ is the root-mean-square of $u'$. The smooth-wall TBL data in Fig. 3(b) shows that the general appearance of the correlation including a streamwise-elongated positive correlation region flanked by a negative correlation region and a distinctive X-pattern with a zero-crossing point at $x/\delta = 3.0$ is very similar to those observed in a previous experimental study of TBLs.[2] The possible helix angle of the correlation depicted by the black dashed lines is approximately ~5°, consistent with the instantaneous field shown in Fig. 2(b). Since the overall pattern of the low-level contour for the correlation can be understood as an imprint of the VLSMs in the flow, the long structures inclined to the spanwise direction with positive and negative angles in the instantaneous fields contribute to form the X-shaped correlation pattern. The present result is consistent with the correlation in a smooth-wall turbulent pipe flow,[8] supporting the contention that the X-shaped correlation pattern is created by the spanwise-inclined streaks with favored helix angles. Compared to that over the smooth-wall, the correlation over the rough-wall in Fig. 3(a) reveals that the helix angle of the correlation is less than 3° in both the upstream and downstream directions with longer streamwise and wider spanwise length scales. Although not shown here, the spectral filtering of the correlations based on the spanwise wavelength of $\lambda_z/\delta > 0.5$ to identify the contribution of the long structures to the correlations provides similar behavior.

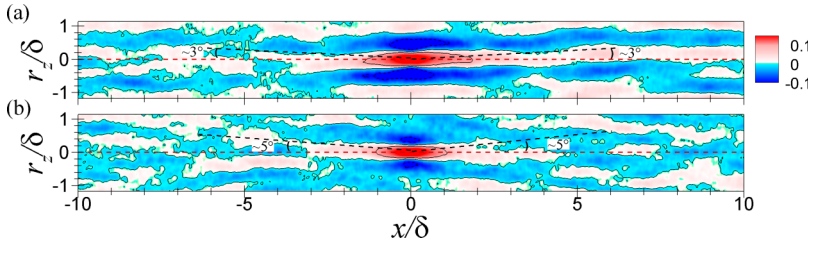


FIG. 3. Streamwise two-point correlation $R_{uu}$ at $y'/\delta = 0.147$: (a) rough- and (b) smooth-wall DNS data. The streamwise reference position $x_r$ for the rough-wall is defined at the center of consecutive rods at $Re_\theta = 1550$. Spanwise symmetric condition, implying reflectional symmetry of $R_{uu}$ with respect to the $r_z/\delta = 0$ line, is not applied in the calculation to show the strong imprint of the patterns of $u'$-structures with helix angles clearly. The contours are varied from −0.1 to 0.1 with an interval of 0.1. Red dashed lines are included to show the zero-crossing point of the contours, and black dashed lines indicate the helix angles of the correlations.

This article is copyrighted as indicated in the article. Reuse of AIP content is subject to the terms at: http://scitation.aip.org/termsconditions. Downloaded to IP: 114.70.8.215 On: Wed, 13 Jan 2016 01:20:18

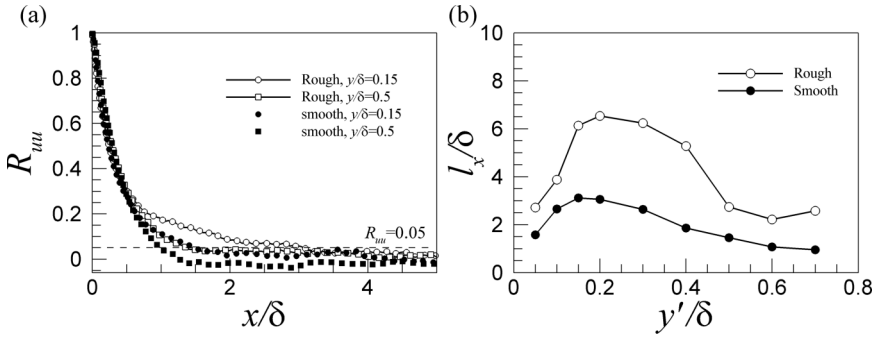


FIG. 4. (a) Streamwise line plot of $R_{uu}$ in the log and wake regions ($y'/\delta = 0.147$ and 0.5) at $r_z/\delta = 0$ and (b) variation of the characteristic streamwise length scale $l_x$ based on the range of streamwise displacement where $R_{uu} > 0.05$.

The wall-normal variations of the streamwise and spanwise length scales over rough- and smooth-walls are shown in Figs. 4 and 5. In one-dimensional plots, two profiles in the log and wake regions are displayed over the rough- and smooth-walls, respectively, to clarify the variation of the outer-layer structures. The length scales are extracted based on the region $R_{uu} > 0.05$ at $x = 0$ and $r_z/\delta = 0$.[6,18] A direct comparison of the streamwise length scale in Fig. 4(b) shows that the streamwise coherence of long structures (the correlation component with a low contour level) is increased over the rough-wall as compared to that over the smooth-wall, even if we measure the length scale of the correlation with a higher contour level (e.g., smaller motions with $R_{uu} = 0.1$, 0.2, and higher values). The difference is magnified in the range of $0.15 \leq y/\delta \leq 0.5$, and the features of the correlations may explain the large differences in the Reynolds stress profiles in the outer layer between the smooth- and rough-surfaces.[14,25] The overall characteristic of the streamwise length scale is consistent with previous experimental studies using the same roughness configuration regardless of its size.[15,16] Furthermore, an increase of the spanwise length scale over the rough-wall in Fig. 5(b) is similar to that in TBLs over 2-D and 3-D roughness elements.[15,11]

In order to explain the streamwise scale growth of the correlation over the rough-wall, we employ a feature extraction algorithm to identify the population trends of the negative $u'$-structures contributing to formation of the correlation.[1,6] It has been suggested that these low-momentum regions are created by the successive alignment of hairpin vortices and hairpin packets.[5,6,8,32] Figure 6 shows the length and width distributions of the identified negative $u'$-structures over the rough- and smooth-walls in the log layer. The ordinate is the ratio of the number of the patches found in each length (width) to the total number of detected patches. The population trend exhibits a slightly large population of longer and wider structures over the rough-wall compared to that over the smooth-wall. Note that the maximum length of the structures is comparable between the rough- and smooth-walls on the order of $O(15\delta)$. Thus, it can be concluded that the longer and wider coherence of the correlations over the rough-wall in Figs. 4 and 5 are due to the large population of the longer and wider $u'$-structures as compared to than the smooth-wall flow.

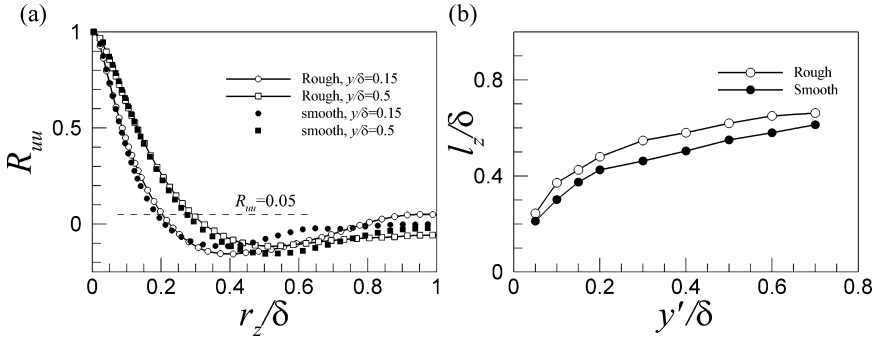


FIG. 5. (a) Spanwise line plot of $R_{uu}$ in the log and wake regions ($y'/\delta = 0.147$ and 0.5) at $x = 0$ and (b) variation of the characteristic spanwise length scale $l_z$ based on the range of spanwise displacement where $R_{uu} > 0.05$.

This article is copyrighted as indicated in the article. Reuse of AIP content is subject to the terms at: http://scitation.aip.org/termsconditions. Downloaded to IP: 114.70.8.215 On: Wed, 13 Jan 2016 01:20:18

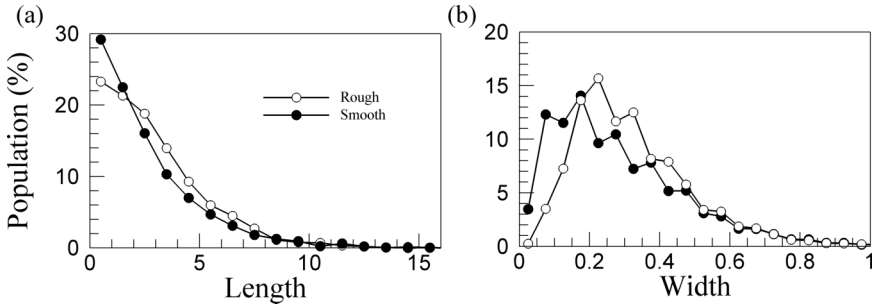


FIG. 6. Population trends of (a) the streamwise length and (b) the spanwise width for low-momentum regions over rough- and smooth-walls at $y'/\delta = 0.147$. The lengths are normalized by the outer scale.

However, there remains an issue for which the mechanism induces longer and wider motions over the rough-wall. In other words, the question is how the long structures are frequently created over the rough-wall. To address this issue of the streamwise scale growth over the rough-wall, time-evolving instantaneous flow fields are examined in detail. The main idea is that small scales organize coherently to create larger scales, as conjectured by Kim and Adrian.[10] For a smooth-wall TBL flow, Lee and Sung[6] and Lee *et al.*[9] successfully demonstrated that this hypothesis is valid with regard to the formation of VLSMs by the concatenation of LSMs in the log layer by instantaneous and statistical analysis.

Figure 7 presents the time-evolution of the instantaneous field shown in Fig. 2(a) to show how the very long negative $u'$-structure with small helix angle is created (the field in Fig. 2(a) corresponds to the snapshot at $t^+ = 25.0$ in Fig. 7). At the initial time of $t^+ = 0$, there are two adjacent structures (black dashed lines) that are not perfectly streamwise-aligned but are spanwise-inclined at two angles of ~4° (the left one) and less than 1° (the right one). The downstream and upstream portions of the left

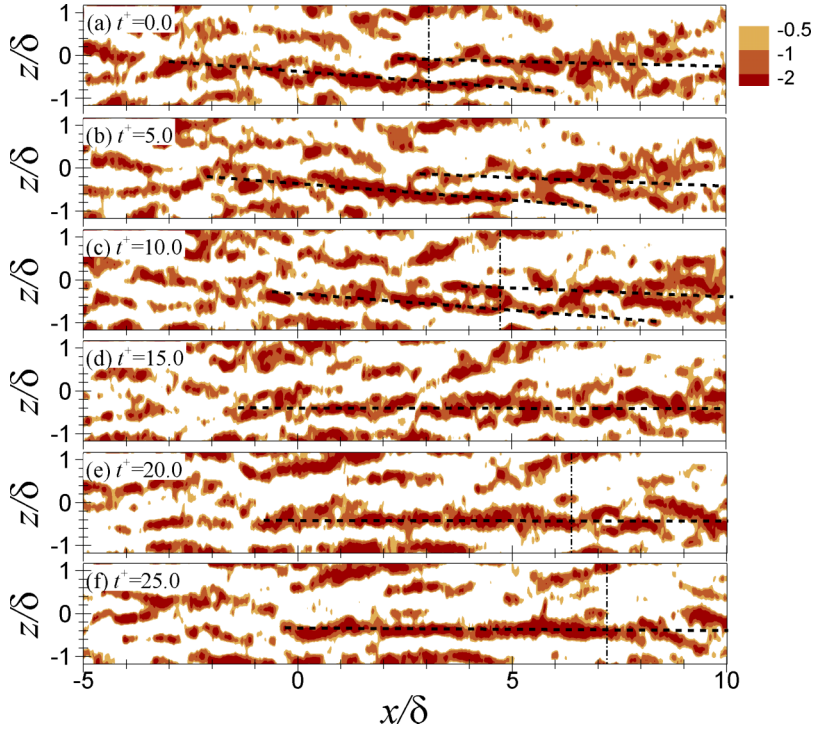


FIG. 7. Time-evolution of the instantaneous fields at $y'/\delta = 0.147$ on the $xz$ plane. The color levels indicate the $-2.0$, $-1.0$, and $-0.5\,u^+$ contours. No spatial filtration is applied. Black dashed lines are included to show the active spanwise merging of two long structures to form a longer structure over the rough-wall. Vertical dashed-dotted lines are present at $t^+ = 0$, 10, 20, and 25 to show the streamwise locations for a further analysis of the structures on the $yz$ plane later.

This article is copyrighted as indicated in the article. Reuse of AIP content is subject to the terms at: http://scitation.aip.org/termsconditions. Downloaded to IP: 114.70.8.215 On: Wed, 13 Jan 2016 01:20:18

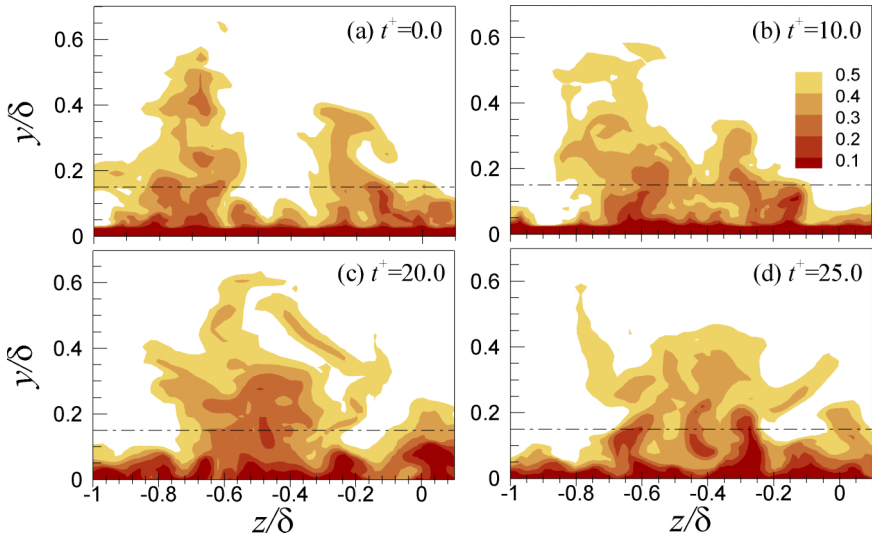


FIG. 8. Time-evolution of the merging structure on the $yz$ plane. The streamwise locations for the structures are shown in Fig. 7 with the dashed-dotted lines. Velocity contours are the streamwise velocities, $U/U_\infty = 0.1$, 0.2, 0.3, 0.4, and 0.5 at $t^+ = 0.0$–25.0. The dashed-dotted lines here depict the log layer ($y'/\delta = 0.15$).

and right structures are overlapped in the streamwise direction, although there is spanwise separation between them. These two structures evolve slowly in time, moving with similar convection velocities along the downstream direction, and there occurs significant spanwise interaction between them, resulting in a streamwise-aligned longer $u'$-structure at $t^+ = 25$. The present observation provides evidence that the active spanwise merging of streamwise-aligned segments of $u'$-structures over the rough-wall can induce longer streamwise-elongated motion with a relatively small inclination in the spanwise direction in the flow.

The spanwise merging signature, creating the streamwise scale growth of the structures, is clearly shown in Fig. 8. The streamwise locations for the $yz$ planes are depicted in Fig. 7 with dashed-dotted lines at four different stages. At $t^+ = 0$, two wall-normal elongated low-momentum regions are distributed with comparable sizes in the spanwise direction (log layer); these motions create low-high-low fluid patterns, consistent with the observation in the correlations. When the interaction of the long structures occurs at a certain downstream position ($t^+ < 10$), the inner sides of these momentum zones gradually merge, indicating that the inner vortices with opposite swirls based on the hairpin vortex model are annihilated, with only the outer vortices with a larger size eventually surviving along the wall-normal direction.[6,7]

In addition to the two-point spatial correlations (Figs. 4 and 5) and population trends (Fig. 6), further evidence for the presence of wider structures over the rough-wall is provided using spanwise energy spectra in Fig. 9, where $k_z$ (= $2\pi/\lambda_z$) is the spanwise wavenumber, $\lambda_z$ is the spanwise wavelength, and $\phi_{uu}$ is the spectral density of $u'$. For the smooth-wall, an energy peak is observed at $y^+ = 15$ with mean spanwise wavelength of the order of 100 in wall units, i.e., a typical signature of the near wall cycle of self-sustained turbulence.[33] The introduction of the rod roughness induces wall-normal shift of the position for the inner peak at around $y^+ = 50$ with maximum wavelength $\lambda_z{}^+ = 200$. In addition, large-scale structure events are strongly energized by the surface roughness in the outer layer, and a secondary outer peak is observed at $y/\delta = 0.2$ with wavelength of $\lambda_z/\delta = 0.8$. The emergence of the outer peak suggests that one of the effects of the surface roughness is to strengthen and/or increase the population of wider structures in the new equilibrium region over the rough-wall.

Because there are many wider structures over the rough-wall based on our documentation, it is reasonable to infer that the possibility of the spanwise merging of structures becomes significant over the rough-wall. This can therefore be a source of the creation of the more frequent spanwise merging for the streamwise scale growth of structures over the rough-wall. The increased spanwise scales of structures over the rough-wall are attributable to large-scale turbulent motions generated by the infinite width of the present roughness, as supported by Volino *et al.*[15] For irregular and random 3-D

This article is copyrighted as indicated in the article. Reuse of AIP content is subject to the terms at: http://scitation.aip.org/termsconditions. Downloaded to IP: 114.70.8.215 On: Wed, 13 Jan 2016 01:20:18

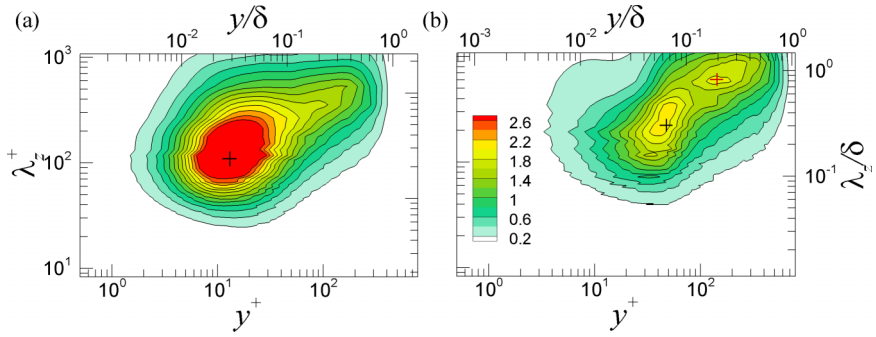


FIG. 9. Premultiplied spanwise energy spectra of the streamwise velocity fluctuations $k_z\phi_{uu}(k_z)$. (a) Smooth-wall and (b) rough-wall at $x/\theta_{in} = 620.5$. The spectra are normalized by $u_\tau^2$. Black cross symbols indicate inner peaks of the spectra, and red cross symbol depicts outer peak of the spectra.

surface roughness, on the other hand, a reduction of the streamwise length scale based on correlations has been reported. Because 3-D surface roughness elements (e.g., the mesh and sand grain roughness) produce turbulent scales of the order of the roughness height, the spanwise scale of structures with large scales is similar to a smooth-wall flow,[11,12] suggesting that the spanwise merging for streamwise scale growth is not significant. The reduced streamwise coherence over the 3-D surface roughness indicates that a break-up of flow structures whose streamwise scales are comparable to the size of the roughness elements plays a dominant role in the formation of the streamwise coherence of the correlation.[11,13]

Before proceeding further, it should be noted that the streamwise scale growth mechanism of the structures over the rough-wall suggested here is distinguishable from the formation mechanism of VLSMs by the continuous alignment of LSMs. One component of the process leading to the large streamwise length of VLSM is the concatenation of adjacent streamwise LSMs caused by the continuous elongation of LSMs due to the strain component of the mean shear. In the present study, however, we provide evidence that the active spanwise merging of LSMs or VLSMs due to the larger width of the structures originating from the roughness induce a longer LSM or VLSM over the rough-wall. Furthermore, it is important to note that the plot in Fig. 7 provides one possible mechanism for the growth of the structure over the rough-wall. In reality, an enormous range of relative flow mechanisms is possible to induce a large streamwise length scale. Because the present DNS data contain very complex vortical structures with large numbers of small-scale vortices, it is difficult to recognize the complete set of vortex dynamics involved in the streamwise scale growth of these structures eye or by systematic image analysis.

In addition to the spanwise merging mechanism for the streamwise scale growth of the structures, we examine the influence of the helix angle and width of the structures on the formation of the coherence of streamwise two-point spatial correlations. Here, a hairpin model revised from the works of Perry and Marusic[34] is considered to construct very long negative $u'$- structures created by the alignment of several LSMs.[6,8–10] In their model, a hairpin (vortex rod) that is rectangular in shape is inclined 45° to the wall in the downstream direction (Fig. 10), and the induced velocity created by the model at a point is calculated based on the Biot-Savart law. The hairpin vortices aligned in the streamwise direction induce a hairpin packet structure, as shown in Fig. 10(a), and the induced velocity within and around the packet in Fig. 10(b) is simply a summation of the velocities induced by individual hairpin vortices.

The concatenation of the packets creates the very long negative streamwise velocity fluctuating structures shown in Fig. 11(a). Here, we assume that the artificial structures are inclined in the spanwise direction with a helix angle of $\alpha = \pm 6°$,[8] and it is expected that the very long scale of the structures can contribute to form a low contour level of correlation (the X-shaped pattern), similar to the correlation in Fig. 3. It is noted that in a previous study, Hutchins and Marusic[2] constructed a sinusoidally wavering synthetic velocity streak (negative $u'$-structure) and showed that such steaks could generate the X-shaped pattern. Figure 11(b) shows a corresponding two-point correlation of the motions in Fig. 11(a). As expected, the correlation shows that a highly elongated positive region is

This article is copyrighted as indicated in the article. Reuse of AIP content is subject to the terms at: http://scitation.aip.org/termsconditions. Downloaded to IP: 114.70.8.215 On: Wed, 13 Jan 2016 01:20:18

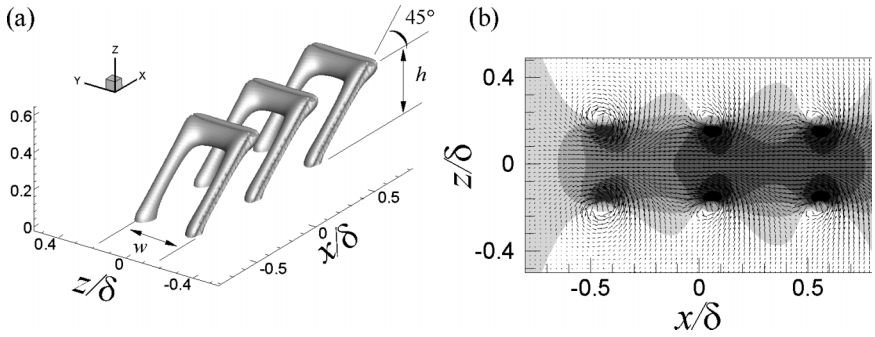


FIG. 10. "Π-shaped" hairpin vortex model of Perry and Marusic.[34] (a) Hairpin vortices aligned in the streamwise direction. The hairpins are inclined toward the flow direction at 45°, creating a hairpin packet, and the width ($w$) and height ($h$) of all hairpins are $0.4\delta$ with a streamwise interval of $0.5\delta$ for simplicity. (b) Vector field induced by the hairpin packet in the horizontal plane at $y/\delta = 0.15$. Grey contours inside the counter-rotating vortices are negative $u'$-fluctuations (low-momentum region) induced by the hairpins and positive $u'$-fluctuations (high-momentum region) are shown outside the hairpins in white.

flanked by negative correlated regions (shown in white) on each side due to vortex induction from the legs and the head, while the correlation is inclined at a helical angle due to the spanwise-inclined very long scales of the structures, creating a distinctive X-shaped pattern. Note that for a higher contour level, streamwise-elongated elliptic contours similar to those in Fig. 3 are also shown. To examine the effect of the helix angle on the correlation, the helix angle of the structures is reduced to $\alpha = \pm 3°$ while the other parameters are fixed. Figure 11(c) shows that the reduction of the helix angle results in significantly increased coherence of the correlation along the $r_z/\delta$ line. Furthermore, Figure 11(d)

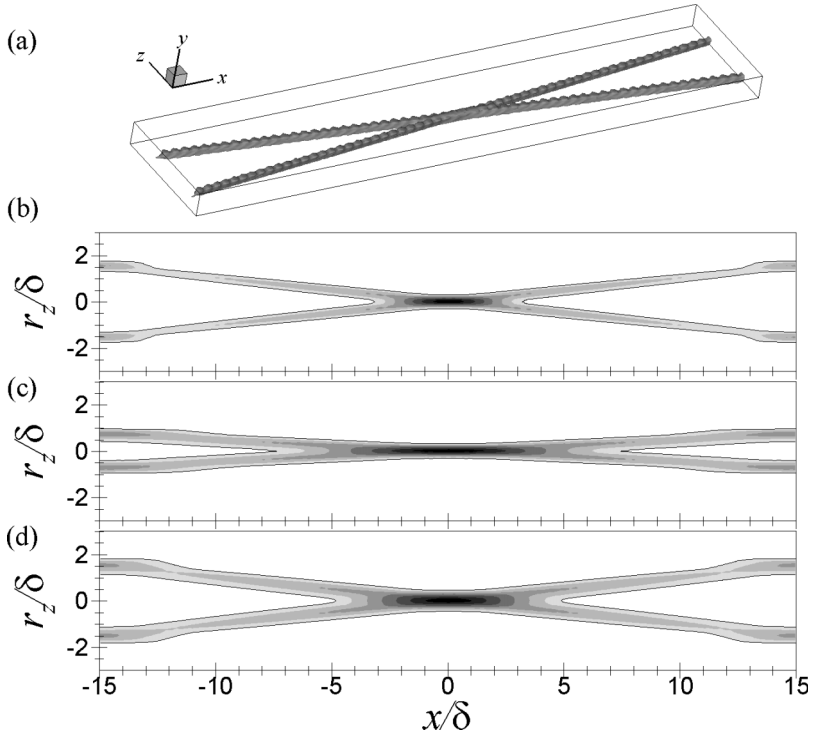


FIG. 11. (a) Artificial very long spanwise-inclined structures constructed by the alignment of "Π-shaped" hairpins ($w = h = 0.4\delta$) with a streamwise interval of $0.5\delta$. The inclination angle of the structures in the spanwise direction is about $\alpha = \pm 6°$. The corresponding streamwise two-point correlation contours $R_{uu}$ are shown in (b). (c) shows the correlation with different helical angles of $\alpha = \pm 3°$ ($w = h = 0.4\delta$) and (d) exhibits the correlation with different widths ($w = 0.6\delta$, $h = 0.4\delta$, $\alpha = \pm 6°$) of the structures compared to (a). The contours in each correlation vary from 0.3 to 1.0 with an interval of 0.1. The lowest contour is shown with solid lines in each figure.

This article is copyrighted as indicated in the article. Reuse of AIP content is subject to the terms at: http://scitation.aip.org/termsconditions. Downloaded to IP: 114.70.8.215 On: Wed, 13 Jan 2016 01:20:18

exhibits that an increase of the spanwise width of the structures compared to those in Fig. 11(a) also introduces longer streamwise coherence of the structures. These results indicate that the structures over the rough-wall characterized by a small helix angle and a large spanwise width can induce a longer streamwise length scale due to their spanwise symmetry in the correlation.

## IV. SUMMARY AND CONCLUSIONS

In the present study, we performed a DNS of a spatially developing TBL flow with regularly arranged 2-D rod surface roughness to investigate the streamwise scale growth mechanism of structures in the logarithmic layer. To avoid the influence of a flow transition from smooth- to rough-walls, the flow fields were analyzed in a new equilibrium region downstream, and the spatial features of the streamwise velocity fluctuating structures over that region were compared with those over a smooth-wall. Inspection of the instantaneous flow fields and streamwise two-point spatial correlations of the streamwise velocity fluctuations showed that the streamwise and spanwise length scales of the structures over the rough-wall are generally larger than those over the smooth-wall, while the spanwise inclination angle to the streamwise direction (helix angle) is smaller over the rough-wall. The increase in the length scales of the correlations was attributed to the large population of longer and wider structures over the rough-wall.

In order to examine how longer structures are created over the rough-wall, time-evolving instantaneous flow fields were analyzed. The results showed that the spanwise merging of long structures over the rough-wall could induce more streamwise-elongated motion with a small helix angle. The larger spanwise length scale over the rough-wall generated by the infinite width of the 2-D roughness indicates that there is more of a possibility for the spanwise merging of the structures over the rough-wall to occur, resulting in a large population of long structures. Based on previous work in which VLSM is induced by a consequence of spanwise offset LSMs,[6,8–10] the influence of the helix angle and spanwise width on the coherence of two-point correlations was explored using a hairpin model. The two-point correlations of the streamwise velocity fluctuations induced by two artificial structures with varying helix angles and widths showed that a small helix angle and a large spanwise width observed over the rough-wall could induce longer coherence of the correlations due to the symmetry of the long structures in the spanwise direction.

## ACKNOWLEDGMENTS

This research was supported by Basic Science Research Program through the National Research Foundation of Korea (NRF) funded by the Ministry of Education (No. NRF-2014R1A1A2057031) and partially by the 2015 Research Fund (No. 1.150033.01 and 1.140070.01) of UNIST.

[1] B. Ganapathisubramani, E. K. Longmire, and I. Marusic, "Characteristics of vortex packets in turbulent boundary layers," J. Fluid Mech. **478**, 35–46 (2003).
[2] N. Hutchins and I. Marusic, "Evidence of very long meandering features in the logarithmic region of turbulent boundary layers," J. Fluid Mech. **579**, 1–28 (2007).
[3] X. Wu, J. R. Baltzer, and R. J. Adrian, "Direct numerical simulation of a 30R long turbulent pipe flow at $R^+ = 685$: Large- and very large-scale motions," J. Fluid Mech. **698**, 235–281 (2012).
[4] J. Jiménez, "The largest scales of turbulent wall flows," in *Annual Research Briefs* (Center for Turbulence Research, Stanford University, 1998), pp. 137–154.
[5] R. J. Adrian, C. D. Meinhart, and C. D. Tomkins, "Vortex organization in the outer region of the turbulent boundary layer," J. Fluid Mech. **422**, 1–54 (2000).
[6] J. H. Lee and H. J. Sung, "Very-large-scale motions in a turbulent boundary layer," J. Fluid Mech. **673**, 80–120 (2011).
[7] C. D. Tomkins and R. J. Adrian, "Spanwise structure and scale growth in turbulent boundary layers," J. Fluid Mech. **490**, 37–74 (2003).
[8] J. R. Baltzer, R. J. Adrian, and X. Wu., "Structural organization of large and very large scales in turbulent pipe flow simulation," J. Fluid Mech. **720**, 236–279 (2013).
[9] J. Lee, J. H. Lee, J.-I. Choi, and H. J. Sung, "Spatial organization of large- and very-large-scale motions in a turbulent channel flow," J. Fluid Mech. **749**, 818–840 (2014).
[10] K. C. Kim and R. J. Adrian, "Very large-scale motion in the outer layer," Phys. Fluids **11**, 417–422 (1999).
[11] P.-Å. Krogstad and R. A. Antonia, "Structure of turbulent boundary layers on smooth and rough walls," J. Fluid Mech. **277**, 1–21 (1994).
[12] R. J. Volino, M. P. Schultz, and K. A. Flack, "Turbulence structure in rough- and smooth-wall boundary layers," J. Fluid Mech. **592**, 263–293 (2007).

This article is copyrighted as indicated in the article. Reuse of AIP content is subject to the terms at: http://scitation.aip.org/termsconditions. Downloaded to IP: 114.70.8.215 On: Wed, 13 Jan 2016 01:20:18

[13] Y. Wu and K. T. Christensen, "Spatial structure of a turbulent boundary layer with irregular surface roughness," J. Fluid Mech. **655**, 380–418 (2010).
[14] J. H. Lee, H. J. Sung, and P.-A. Krogstad, "Direct numerical simulation of the turbulent boundary layer over a cube-roughened wall," J. Fluid Mech. **669**, 397–431 (2011).
[15] R. J. Volino, M. P. Schultz, and K. A. Flack, "Turbulence structure in a boundary layer with two-dimensional roughness," J. Fluid Mech. **635**, 75–101 (2009).
[16] R. J. Volino, M. P. Schultz, and K. A. Flack, "Turbulence structure in boundary layers over periodic two- and three-dimensional roughness," J. Fluid Mech. **676**, 172–190 (2011).
[17] Y. Wu and K. T. Christensen, "Outer-layer similarity in the presence of a practical rough-wall topography," Phys. Fluids **19**, 085108 (2007).
[18] S. C. C. Bailey, M. Hultmark, A. J. Smits, and M. P. Schultz, "Azimuthal structure of turbulence in high Reynolds number pipe flow," J. Fluid Mech. **615**, 121–138 (2008).
[19] R. Mejia-Alvarez, Y. Wu, and K. T. Christensen, "Observations of meandering superstructures in the roughness sublayer of a turbulent boundary layer," Int. J. Heat Fluid Flow **48**, 43–51 (2014).
[20] D. J. C. Dennis and T. B. Nickels, "On the limitations of Taylor's hypothesis in constructing long structures in a turbulent boundary layer," J. Fluid Mech. **614**, 197–206 (2008).
[21] J. C. del Álamo and J. Jiménez, "Estimation of turbulent convection velocities and corrections to Taylor's approximation," J. Fluid Mech. **640**, 5–26 (2009).
[22] K. A. Flack, M. P. Schultz, and J. S. Connelly, "Examination of a critical roughness height for outer layer similarity," Phys. Fluids **19**, 095104 (2007).
[23] K. Kim, S.-J. Baek, and H. J. Sung, "An implicit velocity decoupling procedure for the incompressible Navier-Stokes equations," Int. J. Numer. Methods Fluids **38**, 125–138 (2002).
[24] J. Kim, D. Kim, and H. Choi, "An immersed boundary finite-volume method for simulations of flow in complex geometries," J. Comput. Phys. **171**, 132–150 (2001).
[25] S. H. Lee and H. J. Sung, "Direct numerical simulation of the turbulent boundary layer over a rod-roughened wall," J. Fluid Mech. **584**, 125–146 (2007).
[26] T. S. Lund, X. Wu, and K. D. Squires, "Generation of turbulent inflow data for spatially developing boundary layer simulation," J. Comput. Phys. **140**, 233–258 (1998).
[27] P. R. Spalart, "Direct simulation of a turbulent boundary layer up to $Re_\theta = 1410$," J. Fluid Mech. **187**, 61–98 (1988).
[28] P. S. Jackson, "On the displacement height in the logarithmic profiles," J. Fluid Mech. **111**, 15–25 (1981).
[29] J. H. Lee, "Turbulent boundary layer flow with a step change from smooth to rough surface," Int. J. Heat Fluid Flow **54**, 39–54 (2015).
[30] M. Bernardini and S. Pirozzoli, "Inner/outer layer interactions in turbulent boundary layers: A refined measure for the large-scale amplitude modulation mechanism," Phys. Fluids **23**, 061701 (2011).
[31] J. Ahn, J. H. Lee, S. J. Jang, and H. J. Sung, "Direct numerical simulation of fully developed turbulent pipe flows," Int. J. Heat Fluid Flow **44**, 222–228 (2013).
[32] R. J. Adrian, "Hairpin vortex organization in wall turbulence," Phys. Fluids **19**, 041301 (2007).
[33] R. L. Panton, "Overview of the self-sustaining mechanisms of wall turbulence," Prog. Aerosp. Sci. **37**, 341–383 (2001).
[34] A. E. Perry and I. Marusic, "A wall-wake model for the turbulence structure of boundary layers. Part 1. Extension of the attached eddy hypothesis," J. Fluid Mech. **298**, 361–388 (1995).

This article is copyrighted as indicated in the article. Reuse of AIP content is subject to the terms at: http://scitation.aip.org/termsconditions. Downloaded to IP: 114.70.8.215 On: Wed, 13 Jan 2016 01:20:18